The Effect of Wire History on the Coarsened Substructure and Secondary Recrystallization of Doped Tungsten

C.L. BRIANT, O. HORACSEK, and K. HORACSEK

This article reports a study of primary and secondary recrystallization in tungsten wire. Samples with two different processing histories were annealed in the electron emission microscope, and the recrystallization process was followed. The fibers produced by drawing were first observed to widen and break up into shorter lengths. As the temperature was raised, the secondary recrystallization occurred in a characteristic, stepwise motion, with the secondary grain moving from one position to the next and then remaining pinned at the new position, sometimes for the entire length of the test. It was found that the temperature at which secondary recrystallization occurred depended on the heating rate. If a slow heating rate was used, the temperature at which secondary recrystallization occurred would be higher. This result was interpreted to mean that the slower heating rate allowed more strain to be annealed out of the wire before secondary recrystallization occurred and thus lowered the driving force for this process. The secondary recrystallization temperature could not be correlated with the primary grain structure or differences in the potassium bubble distribution in the wire. The primary recrystallized grain structures of the two wires were also different, and this difference, too, was attributed to differences in the amount of stored energy in the wire at the start of the annealing. It was also shown that even though the bulk potassium content of the two wires was the same and the bubble distributions in the two wires were similar, the bubble distributions in the ingots were different.

I. INTRODUCTION

THE tungsten wire that is used in lamp filaments has a small diameter that is produced by repeated wire drawing. The microstructure of this as-drawn wire is fibrous and consists of long, narrow grains. In this condition, the potassium, which is the key doping material in lamp-quality tungsten, is contained in ellipsoids that have very high aspect ratios.[1-4] The precursors of these ellipsoids are potassium-filled pores in the sintered ingot. After this wire is coiled to make a filament, it must be heated to the operating temperature of the lamp. During this initial heatup, the potassium ellipsoids breakup into bubble rows, and secondary recrystallization occurs. During this latter process, a few grains grow and consume all others present in the material, and the grains that form often occupy the entire wire diameter. Because of the interaction between the growing grains and the bubble rows, the grains that are formed have a wavelike shape, known as an interlocking structure, in which most of the grain boundary is parallel to the wire axis and only small parts of the boundary are perpendicular to it. This type of grain structure allows very little grain boundary sliding at elevated temperatures[5-10] and thus produces a long-life filament. Micrographs of this grain morphology and the bubble rows are shown in References 1 through 3.

Because the shape of the secondary grains is so important in determining filament life, there have been a number of studies examining the process by which the grains are formed.[2,11-17] Most studies have concluded that the potassium bubble size and bubble row length and spacing are the most important factors in determining the shape of the grains. However, there have been a few studies that have indicated that the entire process history of the wire (powder processing, doping, thermomechanical processing, and annealing) can affect the secondary recrystallization temperature and the shape of the secondary grains.[17,18,19] In this article, we report a study of secondary recrystallization in two different tungsten wires. These wires had different process histories, but their bulk potassium concentrations were approximately the same. Our results show that these two wires had different secondary recrystallization temperatures, different morphologies of the secondary grains, and different grain structures after primary recrystallization. We will propose that these wires differ because their thermomechanical processing history was different. The differences did not appear to result from differences in the potassium bubble distribution in the wires. We also found that the secondary recrystallization depended on the way in which we heated the wire to the secondary recrystallization temperature. A slower heating rate produced a higher secondary recrystallization temperature than a fast heating rate.

II. EXPERIMENTAL PROCEDURE

The work was conducted on 0.39-mm-diameter KSiAl-doped lamp-grade tungsten wires prepared from two sintered ingots having similar potassium contents but different distributions of pore sizes. The properties of the ingots are listed in Table I. The wires made from the two ingots were prepared by two different proprietary processing schedules. The two ingots and the two wires made from them will be designated as "A" and "B." After the same, standard treatment that produces secondary recrystallization, the wires have different grain

C.L. BRIANT, Visiting Research Scientist, O. HORACSEK, and K. HORACSEK are with the Research Institute for Technical Physics of the Hungarian Academy of Sciences, H-1325 Budapest, Hungary. C.L. BRIANT is permanently affiliated with General Electric Company, Research and Development Center, Schenectady, NY 12019.

Manuscript submitted June 3, 1992.

aspect ratios. For wire A, the ratio is 11.5, and for wire B, it is 9.

The porosity on the fractured surface of the sintered ingots was investigated by scanning electron microscopy (SEM). Since the high-temperature properties of doped tungsten wires may depend on the smallest, potassium-containing pore population of the ingot,[20] our quantitative evaluation of the ingot porosity was restricted to pore diameters of less than 1 μm. The differences in the size distribution of the pores was characterized by plots that were obtained by measuring the pores on the SEM micrographs and counting their number for the corresponding size ranges. For the development of the plots, 12 randomly chosen areas were taken from each ingot.

Kinetics studies of the secondary recrystallization of the wires were conducted with a simple electron emission microscope (EEM).[21] Prior to insertion into the EEM, the samples were polished in sodium hydroxide. The temperature of the sample in the EEM was increased by self-resistance heating, and the thermally emitted electrons were focused onto the fluorescent screen by an electrostatic lens. The direct observation of the structural changes was allowed by orientation contrast associated with the differences in the work function of the electrons for the different grains. As the grain boundaries moved during our annealing experiments, their new positions were detectable on the screen without delay, since orientation contrast, and not thermal etching, is used to recognize the position of the grain boundaries. In this way, the kinetics of secondary recrystallization could be directly observed and recorded.

Two rates of heating were applied for both the A and B wire samples. In one case, there was a continuous increase within 1 minute to 1600 °C, followed by annealing at this temperature for 3 hours. After this anneal, the temperature was further increased in 100 °C steps until secondary recrystallization began. After each increase of 100 °C, the sample was held at the temperature for 2 minutes. This heating program will be referred to in the text as slow heating. The second heating schedule was similar to the first except the 3-hour anneal at 1600 °C was omitted. The sample was first brought to 1600 °C in 1 minute, and then after 2 minutes, the temperature was increased by 100 °C. From that point on, we followed the same schedule as listed above. This heating schedule will be referred to as rapid heating.

In order for us to observe relatively large parts of the sample surface during secondary recrystallization, the EEM was used at only a few hundred times magnification. After determination of the temperature at which recrystallization began, the sample was removed from the EEM, and the microstructural details of the wire were examined by SEM. In addition, some samples were studied by transmission electron microscopy (TEM). The details of the sample preparation procedure for TEM have been given in Reference 18. Since TEM inherently examines a rather small area of material, we examined in each case samples from two different wires given the same heating rate. We measured the average bubble diameters, the average spacings between the bubble rows, and the average spacings between bubbles in a given row. For each sample, we made between 15 and 30 measurements for each of these parameters. Therefore, for a given heating rate, we made between 30 and 60 measurements.

Table I. Properties of the Two Potassium-Doped Ingots

Ingot	Sintered Density (g/cm^3)	Grain Size (μm)	Potassium Content (Wppm)
A	17.15	6.1	76
B	17.3	6.4	77

III. RESULTS

Although the sintered densities and the potassium contents of the ingots A and B did not differ significantly, the SEM micrographs showed a marked difference in the size distribution of the pore population below 1 μm. Typical SEM fractographs for the two ingots are shown in Figure 1. The distributions of the pore diameters on the fracture surfaces for the two ingots are shown in

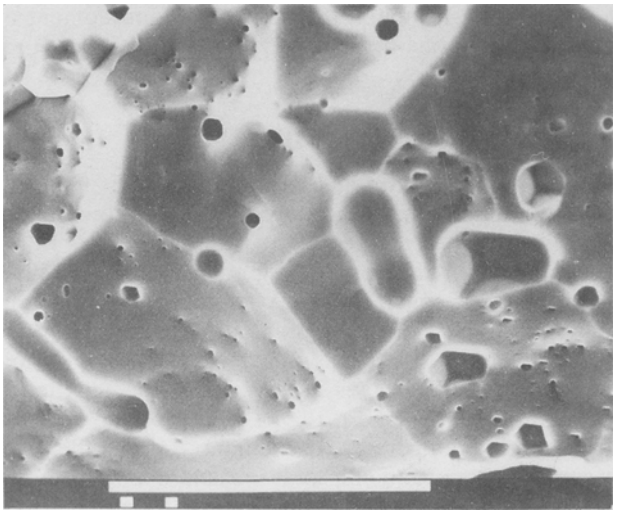

(*a*)

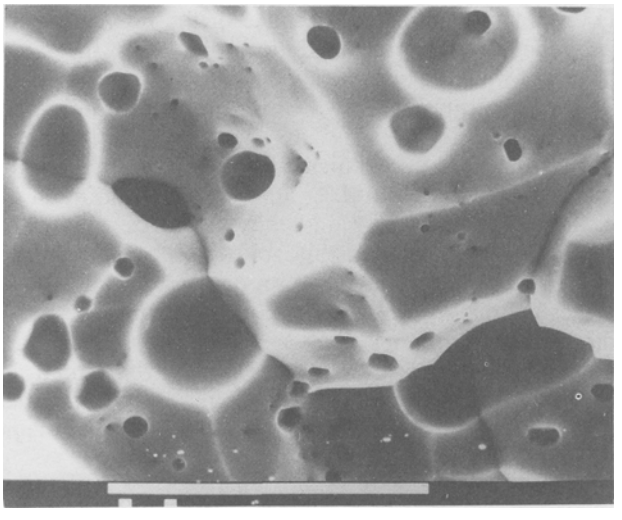

(*b*)

Fig. 1—Scanning electron micrographs from (*a*) ingot A and (*b*) ingot B. The bar on the micrograph represents 10 μm.

Figure 2. Since both the size and the number of the pores can be measured exactly on the SEM micrographs, these plots give correct pictures for the size distributions of the pores. They do not, however, reflect the visible difference in the number density of the pores between the two ingots. Therefore, in Figure 3, we also present two histograms to give additional numerical information concerning the evaluated pore populations. Because of the difficulty of determining the exact surface area of a fracture surface that has a complicated shape, these plots can be considered only as an approximate characterization of the true situation. Thus, on the basis of Figure 3, the number densities of the pores in the two ingots can be compared semiquantitatively. The plots show that there were many more bubbles per unit area with diameters less than 0.1 μm in ingot A than in ingot B.

The primary recrystallization structures of the two wires were different. Figures 4(a) through (d) show histograms for the widths and lengths of the subgrains produced by primary recrystallization for both wires A and B. Different histograms are given for wires that had been slowly heated and wires that had been rapidly heated to secondary recrystallization. Also, Figures 5(a) and (b) show typical micrographs of each of these structures, and Table II gives average values for each condition. This examination showed that the wires were not homogeneous on a fine scale and that reliable averages could be obtained only after hundreds of grains had been counted. All of these results, however, show that wire A had grains that are longer and narrower than wire B. For example, in wire B, the distribution of lengths has a definite peak between 4 and 6 μm, and there were many fewer grains with lengths greater than 10 μm. In contrast, for both length histograms for wire A, the category with the greatest number of entries was that denoted as greater than 15 μm. For the samples of wire A that were rapidly heated, there was no obvious peak in the distribution of lengths less than 15 μm, and for the slowly heated sample, there was only a slight peak in the distribution between 3 and 6 μm. All of the histograms of the widths are more strongly peaked than those for the lengths. For wire A, the distribution is peaked between 0.6 and 0.8 μm for both heating rates. For wire B, the peak in the distribution is between 0.8 and 1.2 μm for both heating rates, and there was a higher percentage of fibers with widths greater than 1.2 μm in wire B than in wire A.

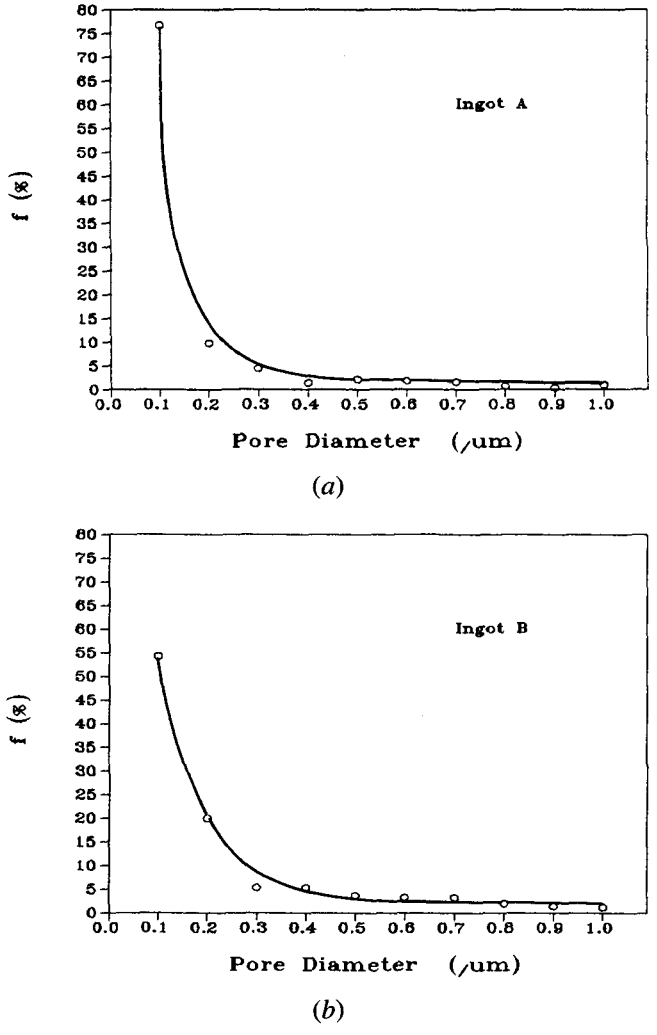

Fig. 2—Frequency distribution of the pore diameters in (*a*) ingot A and (*b*) ingot B.

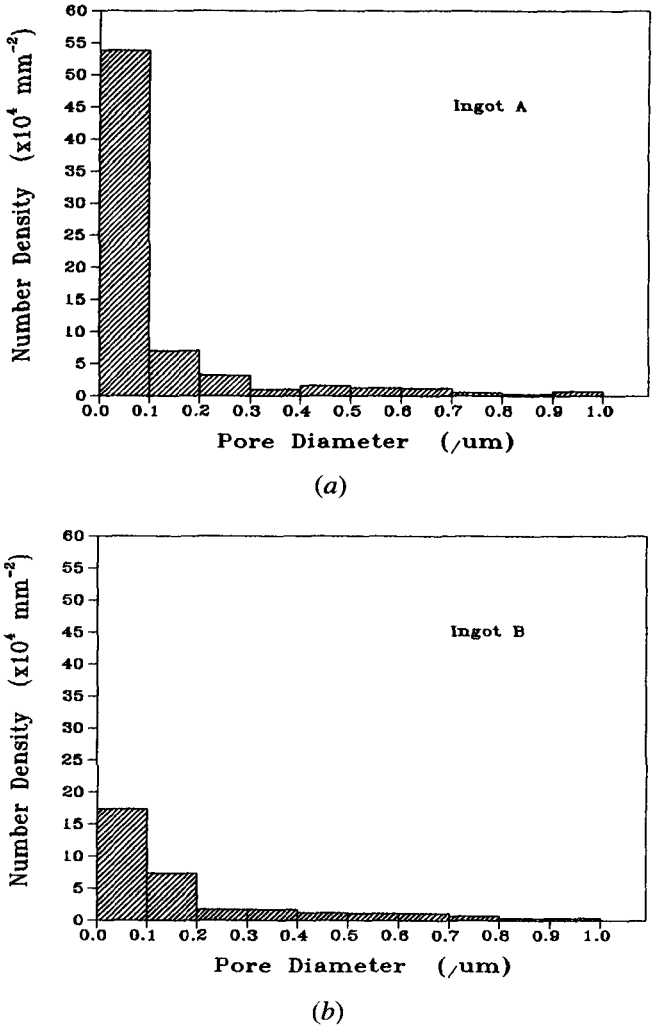

Fig. 3—Histograms showing the number density of pores as a function of size in (*a*) ingot A and (*b*) ingot B.

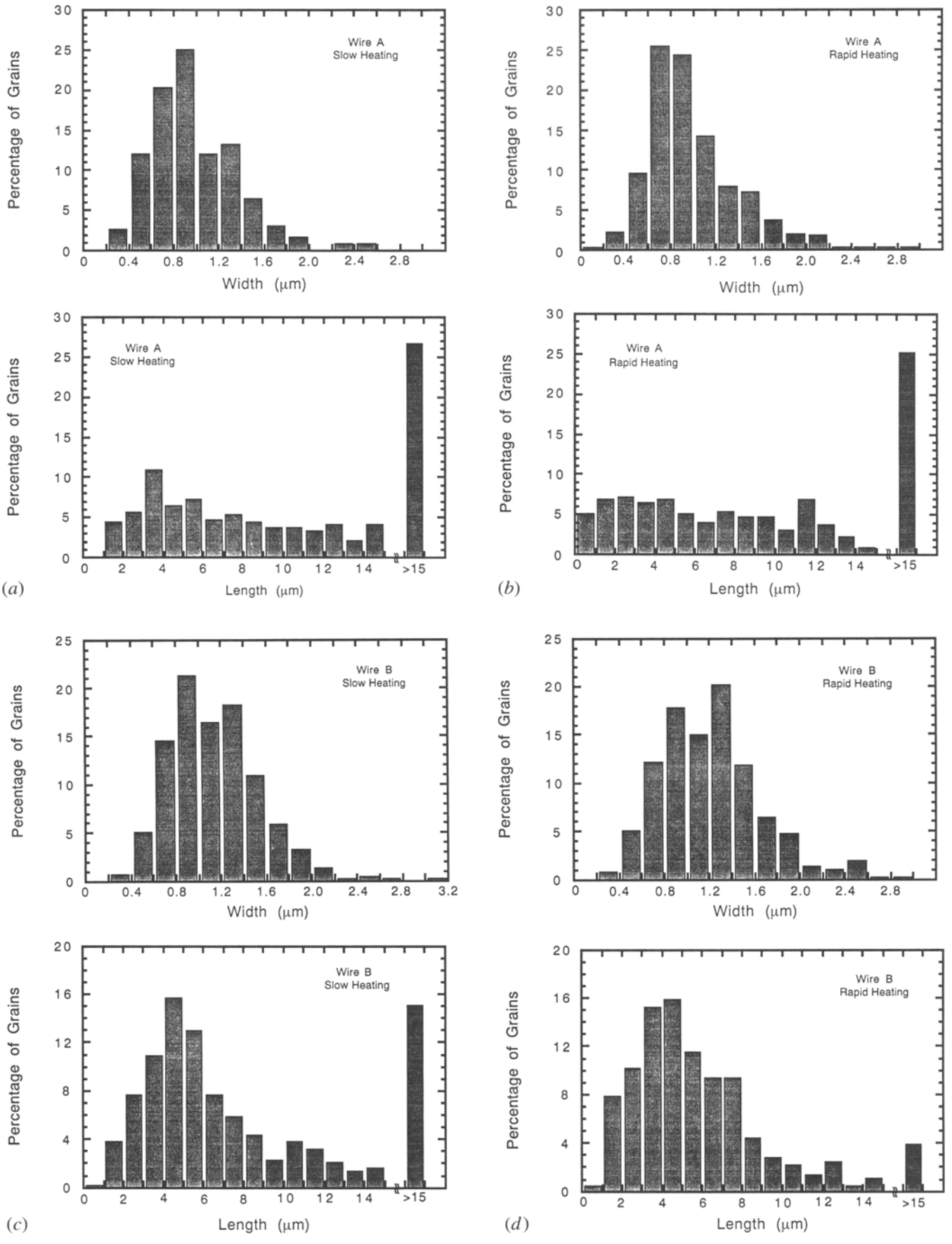

Fig. 4—Histograms showing the widths and lengths of the grains produced by primary recrystallization in the two wire types given two different heating rates. Each histogram was constructed using over 100 measurements for the different wires and heating schedules: (*a*) wire A, slow heating; (*b*) wire A, rapid heating; (*c*) wire B, slow heating; and (*d*) wire B, rapid heating.

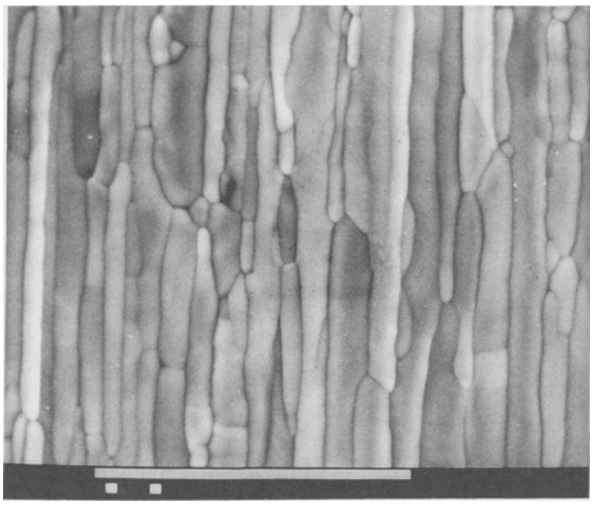

(*a*)

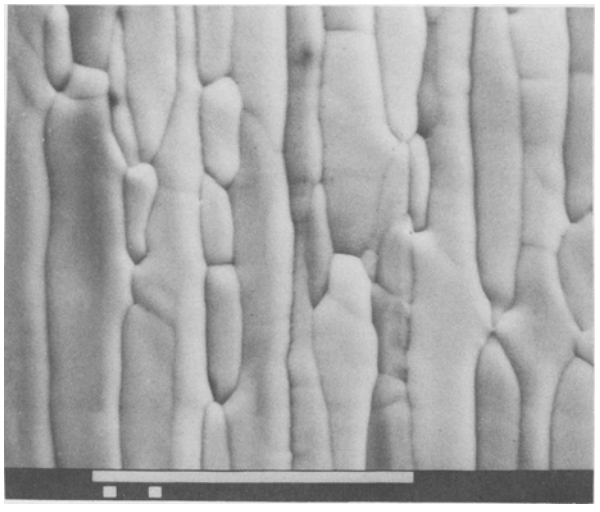

(*b*)

Fig. 5—Scanning electron micrographs showing the grain structure produced by primary recrystallization in (*a*) wire A and (*b*) wire B. The micron marker represents 10 μm.

Although there were clear general differences between wires A and B, we found, as already indicated, much smaller differences in the primary structure of the same wire for the two different heating rates. The average values in Table II and the histograms show that the slower heating produced slightly narrower fibers than the fast heating rate for both wires. For wire B, the slower rate produced a longer fiber as well, but for wire A, the difference in lengths seemed to be insignificant. For the slower heating rate for wire A, we counted more grains with lengths greater than 15 μm, but we also counted more grains with lengths between 3 and 6 μm.

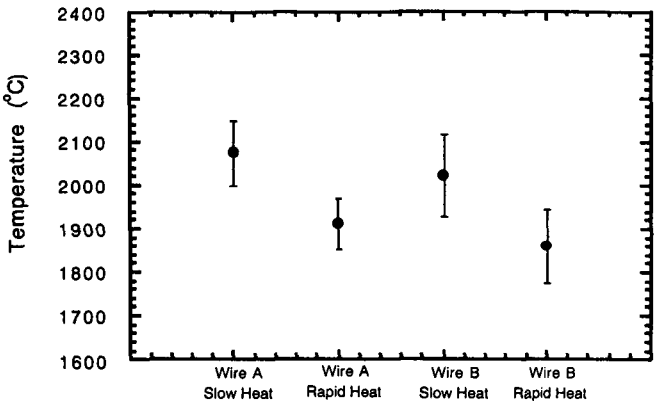

Fig. 6—The secondary recrystallization temperatures for wires A and B given the two different heating schedules.

We found that the secondary recrystallization temperatures of wire A and B were different and that both were affected by the heating rate. Figure 6 shows the results; the values are the average of 10 tests. For both wires, annealing at 1600 °C caused an increase in the secondary recrystallization temperature of approximately 100 °C to 150 °C. For both heating rates, wire A had a higher secondary recrystallization temperature than wire B. For the fast heating rate, the difference was approximately 100 °C, and for the slow heating rate, the difference was approximately 75 °C.

We wanted to determine if there was any correlation between the primary grain structure and the secondary recrystallization temperature. Wire A had the higher recrystallization temperature and grain aspect ratio for both heating rates and had narrower and longer primary grains. But the different heating rates produced few differences in the primary grain structure for the same wire, so we could not explain the increase in the secondary recrystallization temperature caused by a change in heating rate with a change in the primary grain structure. Also, the slowly heated wire B had a higher secondary recrystallization temperature than the rapidly heated wire A, but the rapidly heated wire A had longer and thinner grains. We can conclude that a wire that forms long and thin grains during primary recrystallization may tend to have a higher secondary recrystallization temperature and greater aspect ratio of the secondary grains but that this recrystallization temperature depends on other factors as well.

Table II. The Effect of Wire Type and Heating Rate on Fiber Dimensions and Secondary Recrystallization Temperature

Wire	Heating Rate	Fiber Width (μm)	Fiber Length (μm)	Secondary Recrystallization Temperature (°C)
A	slow	0.91 ± 0.38	9.4 ± 5	2075 ± 75
A	fast	1.0 ± 0.4	10.0 ± 6	1912 ± 58
B	slow	1.1 ± 0.3	7.8 ± 4	2030 ± 91
B	fast	1.2 ± 0.4	5.8 ± 3	1860 ± 87

By using the EEM we were able to obtain more details about the primary and secondary recrystallization processes. We observed, by watching secondary recrystallization on the EEM screen, that there were certain characteristics of this process that were common to both wires. Figures 7(a) through (d) show four micrographs taken at increasing temperatures that typify the various types of structures observed. When the samples were first heated to temperatures below the secondary recrystallization temperature, it was clear that the fibers broadened considerably. At the same time that they broadened, they broke up into shorter lengths. This process manifested itself on the orientation-dependent EEM pictures in the appearance of shorter and wider grains exhibiting different electron emission. Therefore, the microstructure at the onset of secondary recrystallization consisted of coarsened subgrains of very different aspect ratios ranging from practically 1 to even higher than 50. As described above, the actual lengths and widths of the subgrains differed for the two materials, but this general process was always the same. When secondary recrystallization occurred, it happened by a characteristic stepwise motion. The boundary of the secondary grain moved from one position to the next and then remained pinned at the new position, sometimes for the entire length of the test. The pinning appeared to occur in both the radial and axial directions, and the pinning sites were clearly the primary grain boundaries. The extent of the barriers which hindered the movement of the grain boundaries could be correlated with the length and width of the previously coarsened subgrains. Thus, the secondary grains in wire A were more interlocking than those in wire B, apparently because the primary structure of wire A consisted of longer and thinner grains. This point is shown schematically in Figure 8, where we show how the boundary between the secondary grain could reflect the primary grain structure. In most cases, the secondary grain would cover the entire viewing area in the direction of the wire axis, but it would not cover the entire diameter of the wire. Also, we generally found that after the first secondary grain appeared, we had to wait for several minutes or increase the temperature even more before further grain boundary movement was observed. We always found that the boundary between the secondary grains and the part of the sample that had not gone through secondary grain growth consisted of a ledgelike structure, as shown in Figure 9, and that the length and spacing of these ledges was similar to the primary grain structure. Thus, it would appear that, in some places, the boundaries were blocked in their motion by pinning sites and, in other cases, they could break through. In general, the ledge lengths were longer for wire A than for wire B.

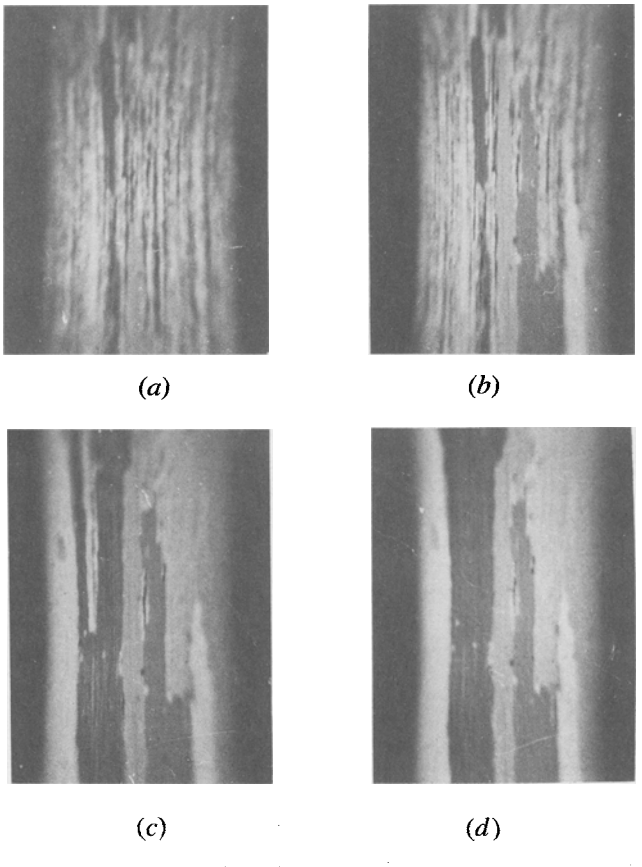

Fig. 7—Electron emission micrographs showing the coarsened substructure present in the wire at the beginning of secondary recrystallization. In this series, one can observe the development of the secondary grains from the primary substructure. Note that the series from (*a*) through (*d*) represents increasing temperature.

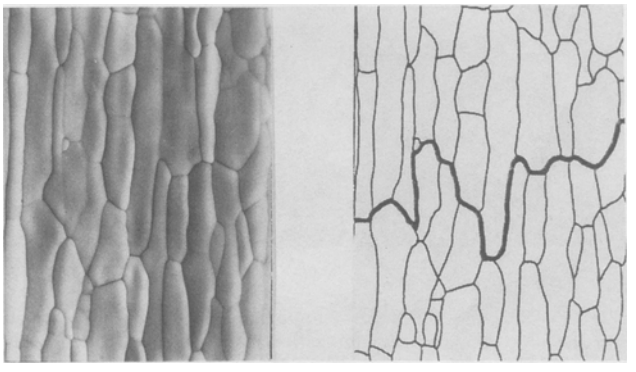

Fig. 8—A schematic showing how the morphology of the primary grains could affect the morphology of the secondary grains if the primary grain boundaries act as pinning points for the secondary grains as they grow.

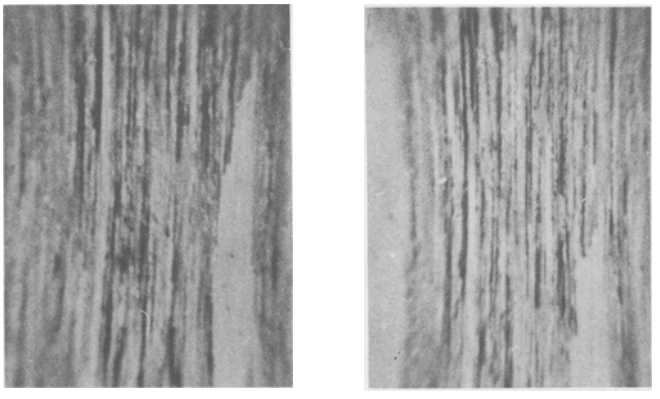

Fig. 9—Electron emission micrographs showing the ledges in the secondary grain structure.

Table III. Data Obtained from Transmission Electron Microscopy on Bubble Row Spacing, Spacing between Bubbles within the Rows, and Bubble Diameters

Wire Type	Heating Rate	Spacing between Bubble Rows (μm)	Spacing between Bubbles in Rows (μm)	Average Bubble Diameter (μm)	Minimum and Maximum Values of Bubble Diameters (μm)
A	slow	0.17 ± 0.12	0.14 ± 0.07	0.031 ± 0.013	0.017 to 0.062
A	slow	0.32 ± 0.2	0.16 ± 0.06	0.037 ± 0.014	0.015 to 0.069
A	rapid	0.16 ± 0.08	0.07 ± 0.04	0.021 ± 0.013	0.007 to 0.038
A	rapid	0.16 ± 0.12	0.08 ± 0.04	0.026 ± 0.016	0.007 to 0.054
B	slow	0.21 ± 0.13	0.13 ± 0.06	0.033 ± 0.017	0.010 to 0.071
B	slow	0.20 ± 0.16	0.14 ± 0.07	0.033 ± 0.010	0.020 to 0.053
B	rapid	0.18 ± 0.14	0.17 ± 0.13	0.041 ± 0.027	0.011 to 0.081
B	rapid	0.12 ± 0.07	0.09 ± 0.05	0.024 ± 0.021	0.009 to 0.063

We also examined by TEM the potassium bubbles in each wire given the two different heating rates. As mentioned above, two samples of each wire heated by the two different schedules were studied, and the results are summarized in Table III. The bubbles were generally arranged in long rows, as shown in Figure 10, although in the slowly heated samples, a few bubbles were situated out of these rows. In general, we found that the bubble diameters, the bubble row spacings, and the distance between the bubbles in a given row did not significantly depend on the wire type and heating rate. However, the following points should be noted. First, we could not make an accurate assessment of the bubble row lengths because we had to use such high magnifications to observe the bubble rows. In almost all cases, they extended beyond the field of view in the micrographs. Second, there was as much scatter between the pairs of samples given identical treatments as there was between samples of the different wires or the samples given the different heating schedules. Third, there was a correlation between the average bubble diameter and the spacing between the bubbles in the rows. This point is shown graphically in Figure 11. Although the error bars are large, there is a clear dependence of the average values on one another. This result is reasonable, since the number of bubbles formed from an ellipsoid of a given size will depend on the wavelength of the perturbation that leads to its breakup.[1,22] As the number of bubbles formed from an ellipsoid decrease, their size and spacing should increase. Fourth, although the average diameters of the bubbles were the same, within the scatter of the data, maximum and minimum values of the bubble diameters listed in the last column of Table III suggested that the rapidly heated samples contained some smaller diameter bubbles that were not present in the slowly heated samples. Thus, there may be some subtle differences in the bubble statistics that would not show up in data that have such a large standard deviation about the average values.

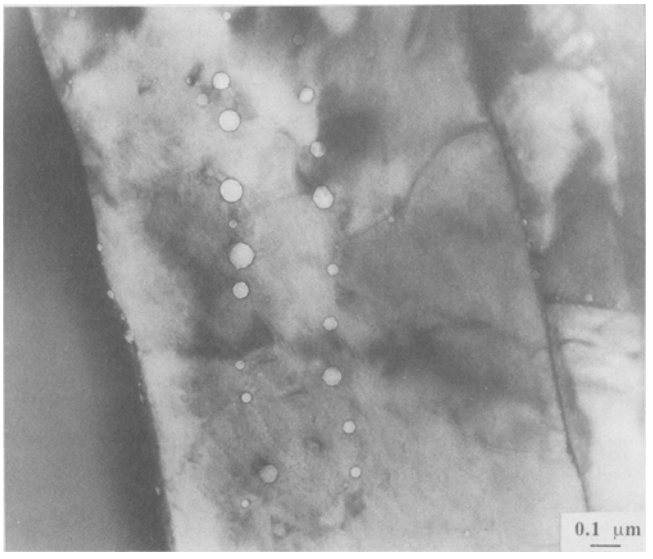

Fig. 10—A typical transmission electron micrograph showing bubble arrangement in a KSiAl-doped wire. This example is of a slowly heated wire A.

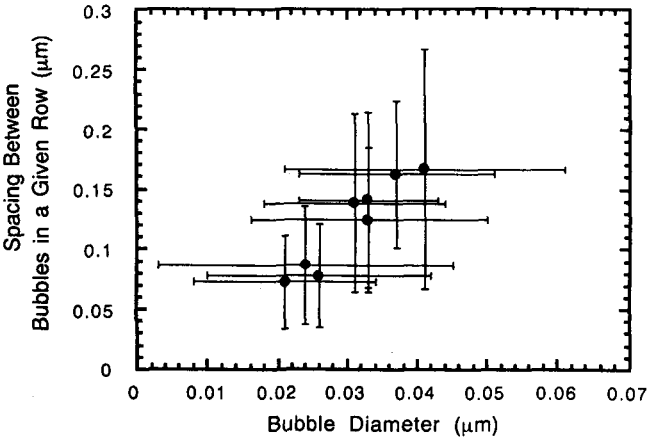

Fig. 11—The average between potassium bubbles in a row plotted as a function of the average bubble diameter. The averages were made from all measurements taken on a given sample prepared for transmission electron microscopy.

IV. DISCUSSION

In the previous section, we presented results for two different wires. Figures 2 and 3 show that wire A was produced from an ingot that had a high number density of small potassium pores, whereas wire B was produced from an ingot with fewer small pores. During primary

recrystallization, wire A formed grains with a higher aspect ratio than wire B, and wire A had a higher recrystallization temperature and more elongated secondary grains than wire B. However, the size and distribution of potassium bubbles in the two wires, with the possible exception of bubble row length, were identical within experimental scatter, as were the potassium concentrations and densities. In both wires, the secondary recrystallization temperature was lower if a rapid heating rate was used.

Let us begin our discussion by considering the primary recrystallization. In the literature on drawn tungsten, the usage of the term "primary recrystallization" is different from its normal use; in the latter case, the term describes the process in which new, strain-free grains nucleate and grow. Through their growth, these new grains consume the worked material. When a drawn tungsten sample is heated, the first step that occurs is polygonization, in which the dislocations in the grains and in the cell walls formed by drawing are organized into low-angle grain boundaries. During this process, many boundaries transverse to the drawing direction are formed. As the temperature is raised, more sections of grain boundaries parallel to the wire axis move across the wire. This movement is usually stopped either by a row of potassium bubbles or by another high-angle grain boundary. This movement also creates transverse grain boundaries, since only sections of these longitudinal grain boundaries move. Once this motion is complete, the process termed "primary recrystallization" is over. The microstructure of this material consists of grains with lower aspect ratios than those present in the drawn material and with the dislocations largely arranged in low-angle boundaries. Because of this resulting structure, this process has simply been referred to as polygonization by some authors.[18,19] As the sample is heated further, secondary grain growth or recrystallization occurs. During this process, a small percentage of the grains grow and consume all of the others.

Previous studies of primary and secondary recrystallization in drawn tungsten have emphasized the importance of the bubbles in controlling grain boundary motion and the final grain structure.[12–16,23,24] These bubbles are undoubtedly important because, without them, the final structure consists of equiaxed grains.[25] However, recent work on the rolled and swaged tungsten rod has shown that the amount of deformation that the tungsten receives also affects both the temperature at which secondary recrystallization occurs and the size of the secondary grains.[18,19] As the amount of deformation that the material receives increases prior to the annealing treatment that will produce the primary and secondary recrystallization, the temperature for secondary recrystallization will decrease, and the resulting grain size will be smaller.

Let us now consider the two wires used in this study. When the wires are heated to 1600 °C, primary recrystallization occurs. In wire A, the aspect ratio of the primary grains is greater than it is in wire B. The first supposition might be that this difference occurs because the number density of the potassium bubbles in wire A is higher and the rows are more closely spaced. However, this difference could not be demonstrated by TEM. We know that the ease with which the grain boundary can overcome the pinning sites will depend on the amount of stored energy produced by the deformation. Given that the potassium bubble distribution in the two wires is similar, we must conclude that the amount of energy stored in wire A is less than that in wire B and that, in wire B, the driving force produced by this additional energy allows the boundaries to overcome the pinning obstacles more easily and thus produce the wider grains.

One can use the same argument to explain the effect of heating rate on secondary recrystallization. For the rapidly heated samples, wire B has a lower secondary recrystallization temperature because there is more stored energy in the material from deformation that can combine with the thermal energy to allow the process to occur. It also then is clear why the hold at 1600 °C for 3 hours raises the secondary recrystallization temperature. This hold allows much of the stored energy produced by the deformation to be annealed out. It then cannot contribute to causing secondary recrystallization, and the thermal energy required to initiate this process must be increased. The fact that the anneal at 1600 °C does not eliminate the difference between the two materials might be explained in two ways. First, there could still be some residual deformation energy remaining in the wire after the anneal and that amount could be different for wires A and B. Second, since the stored energy in both wires must decrease significantly, slight differences in the bubble structures between the wires could become more important and cause the difference in the recrystallization temperature. For example, the data in the last column of Table III suggest that limited bubble coarsening may take place during the slow anneal, and wire A seems to be more sensitive to it.

The final point that we wish to discuss is the fact that the ingots of these two materials had different pore size distributions, whereas the two wires did not show significant differences in their bubble structures. There are two reasons why this result could occur. First, while the size of the bubbles in the wires is determined unambiguously by their potassium content, the potassium pores in the ingot are not necessarily at their equilibrium size.[26] Their size will depend not only on the potassium distribution in the powder but also on how the ingot has been sintered. Therefore, the size distribution of the pores does not reflect reliably the true potassium distribution in the ingot. Second the processing of these two ingots was different both in the temperatures and placement of anneals during processing.

It can also be assumed that the initially very fine potassium distribution in ingot A is more liable to coarsen during the thermomechanical processing and/or the early stage of wire annealing than the relatively low potassium dispersion in ingot B. For example, the potassium content of two or more potassium pores situated very close to each other in ingot A can be joined together by mechanical coalescence during working. In this way, the initial difference in the potassium distribution between the two ingots may decrease, contributing to the development of similar bubble structures in the wires. Unless mechanical processing is identical, it may be difficult to use differences in the pore size distribution in the ingot to predict differences in the bubble distribution in the wire.

V. CONCLUSIONS

The following conclusions can be made from this study:

1. The primary and secondary grain structure and the secondary recrystallization temperature of two wires processed by different schedules and with the same potassium contents and ingot densities were different.
2. It was suggested that this difference arose from differences in the amount of stored energy present in the material when wire drawing was complete. The wire with the lower secondary recrystallization temperature and the wider primary grains should have the greater amount of stored energy, because this energy would assist grain boundary motion in both cases.
3. An anneal of 3 hours at 1600 °C raises the secondary recrystallization temperature in both wires. It is proposed that this increase occurs because the anneal removes much of the stored energy from the deformation.
4. Electron emission microscopy investigations of the secondary recrystallization process of doped tungsten wires showed that grain growth happens by a characteristic stepwise motion, where the extent of the barriers which hinder the migration of the grain boundaries correlates with the length and width of the previously coarsened subgrains.
5. Differences in the size distributions of the pores in ingots cannot necessarily be used to predict differences in bubble distributions in wires unless the process schedule is identical.

ACKNOWLEDGMENTS

The authors would like to acknowledge many helpful discussions with Dr. L. Bartha and Dr. I. Gaal of the Institute for Technical Physics of the Hungarian Academy of Science during the course of this work. They would also like to thank Mr. Michael Larsen of the General Electric Company Research and Development Center for performing the TEM would like to thank the Institute for Technical Physics of the Hungarian Academy of Science for their assistance in this work, which was performed while he was a guest at the Institute.

REFERENCES

1. D.M. Moon and R.C. Koo: *Metall. Trans.*, 1971, vol. 2, pp. 2115-22.
2. David B. Snow: *Metall. Trans. A*, 1976, vol. 7A, pp. 783-794.
3. C.L. Briant: *Proc. 5th Int. Tungsten Symp.*, Budapest, 1990, MPR Shrewsbury, United Kingdom, 1991, p. 169.
4. M.R. Vukcevich: *Proc. 5th Int. Tungsten Symp.*, Budapest, 1990, MPR Shrewsbury, United Kingdom, 1991, pp. 157-168.
5. D.M. Moon and R. Stickler: *High Temp.-High Pressures*, 1971, vol. 3, pp. 503-516.
6. J.W. Pugh: *Metall. Trans.*, 1973, vol. 4., pp. 533-38.
7. R. Raj and G.W. King: *Metall. Trans. A*, 1978, vol. 9A, pp. 941-46.
8. P.K. Wright: *Metall. Trans. A*, 1978, vol. 9A, pp. 955-963.
9. O. Horacsek: *Proc. Inst. Electr. Eng.*, 1980, vol. 127A, pp. 136-41.
10. J.W. Pugh and W.A. Lasch: *Metall. Trans. A*, 1990, vol. 21A, pp. 2209-14.
11. G.D. Rieck: *Acta Metall.*, 1961, vol. 9, pp. 825-32.
12. O. Horacsek: *Z. Metallkd.*, 1972, vol. 63, pp. 269-73.
13. K.C. Thompson-Russell: *Planseeber. Pulvermet.*, 1974, vol. 22, pp. 155-64.
14. H. Warlimont, G. Necker, and H. Schultz: *Z. Metallkd.*, 1975, vol. 66, pp. 279-86.
15. P. Schade: *Planseeber, Pulvermet.*, 1976, vol. 24, pp. 243-53.
16. H.P. Stüwe: *Metall. Trans. A*, 1986, vol. 17A, pp. 1455-59.
17. H.H.R. Jansen: *Philips J. Res.*, 1987, vol. 42, pp. 3-14.
18. C.L. Briant and E.L. Hall: *Metall. Trans. A*, 1989, vol. 20A, pp. 1669-86.
19. C.L. Briant, F. Zaverl, and E.L. Hall: *Mater. Sci. Technol.*, 1991, vol. 7, pp. 923-36.
20. O. Horacsek, Cs. Toth, I. Gaal, and K. Horacsek: *Proc. 12th Plansee Seminar*, 1989, Reutte, Austria, vol. 1, pp. 513-21.
21. O. Horacsek: *Acta Techn. Acad. Sci. Hung.*, 1971, vol. 71, pp. 31-37.
22. C.L. Briant: *Metall. Trans. A*, 1989, vol. 20A, pp. 179-84.
23. S. Friedman and J. Brett: *Metall. Trans.*, 1970, vol. 1, pp. 3225-31.
24. S. Yamazaki, S. Ogura, Y. Fukazawa, and N. Hatae: *High Temp.-High Pressures*, 1978, vol. 10, pp. 329-39.
25. D.B. Snow: *Metall. Trans.*, 1974, vol. 5, pp. 2375-81.
26. J.L. Walter, K.A. Lou, and M.R. Vukcevich: *Proc. 12th Plansee Seminar* 1989, Reutte, Austria, vol. 1, pp. 493-512.